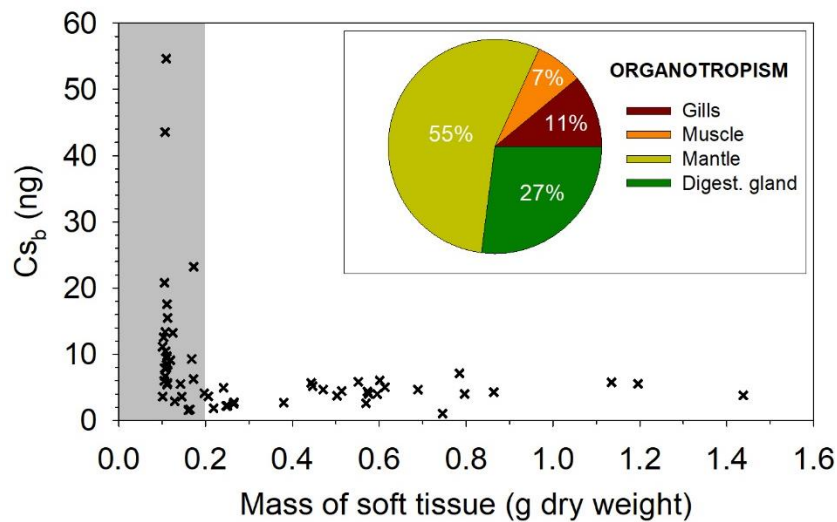


# Reactivity and bioconcentration of stable cesium in a hyperturbid fluvial-estuarine continuum: a combination of field observations and geochemical modelling

Teba Gil-Díaz<sup>a,b\*</sup>, Frédérique Pougnet<sup>a</sup>, Maëva Labassa<sup>a</sup>, Lionel Dutruch<sup>a,c</sup>, Melina Abdou<sup>a</sup>, Alexandra Coynel<sup>a</sup>, Frédérique Eyrolle<sup>d</sup>, Nicolas Briant<sup>e</sup>, Joël Knoery<sup>e</sup>, Jörg Schäfer<sup>a</sup>

<sup>a</sup>Univ. Bordeaux, CNRS, Bordeaux INP, EPOC, UMR 5805, F-33600 Pessac, France; <sup>b</sup>Currently at: Institute of Applied Geosciences, Karlsruhe Institute of Technology, Germany; <sup>c</sup>Currently at: Université de Rennes, UMR CNRS 6118, Campus Beaulieu 35000 Rennes, France; <sup>d</sup>Institut de Radioprotection et de Sûreté Nucléaire (IRSN), PSE-ENV, STAAAR/LRTA, BP 3, 13115 Saint-Paul-lez-Durance, France; <sup>e</sup>Ifremer, CCEM Contamination Chimique des Écosystèmes Marins, F-44000 Nantes, France. \*Corresponding author: teba.gil-diaz@kit.edu



**Figure S1:**  $Cs_b$  content in whole body tissue of wild oysters ( $Cs_b$ , crosses,  $n = 55$ ). Grey area shows  $Cs_b$  variability for soft tissue masses < 200 mg. Inset contains the average distribution of  $Cs_b$  (pooled  $n = 5$ ) in four organs from wild oysters in La Fosse (LF\_85km).

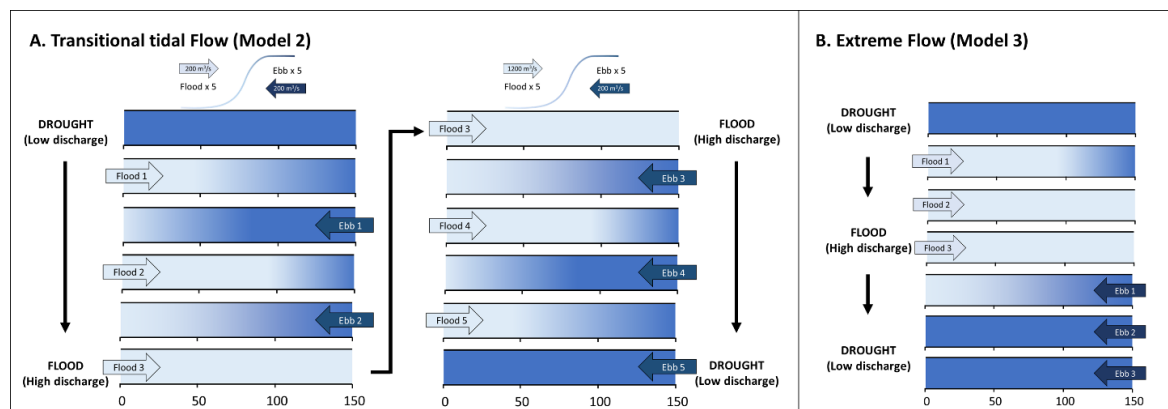


**Figure S2:** Visual scheme of water flow regimes used during modelling approaches. The model names (Model 2 and Model 3) are to be compared with descriptions in Table 1.

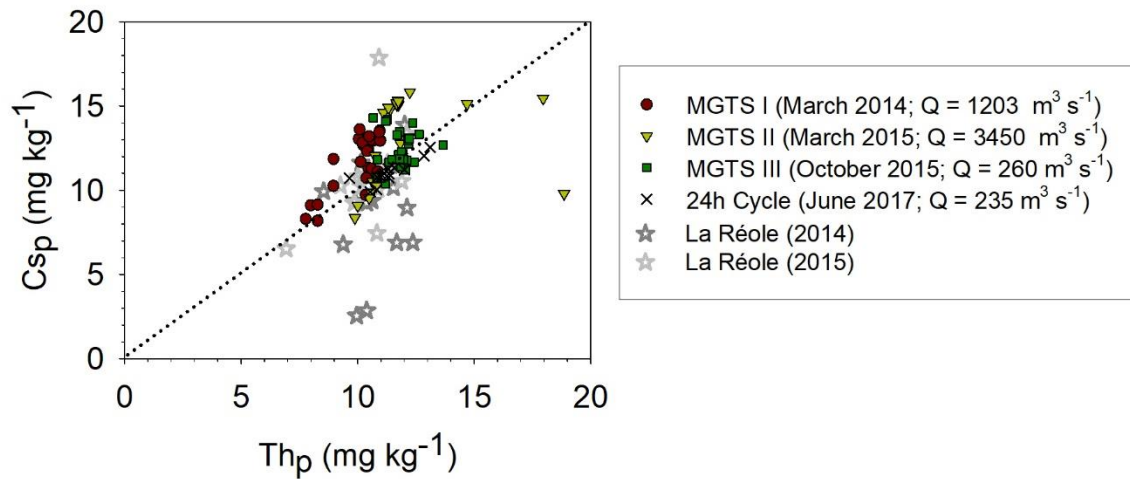


**Figure S3:** Comparison between  $C_{sp}$  and  $Th_p$  concentrations from the estuarine system (along the salinity gradient during the MGTS campaigns between Bdx\_0km and C\_110km, as well as at the estuary mouth during the 24h cycle, site C\_110km). In grey, values from the freshwater endmember at La Réole (LR\_Gar-70km) are also included for two years as an example.

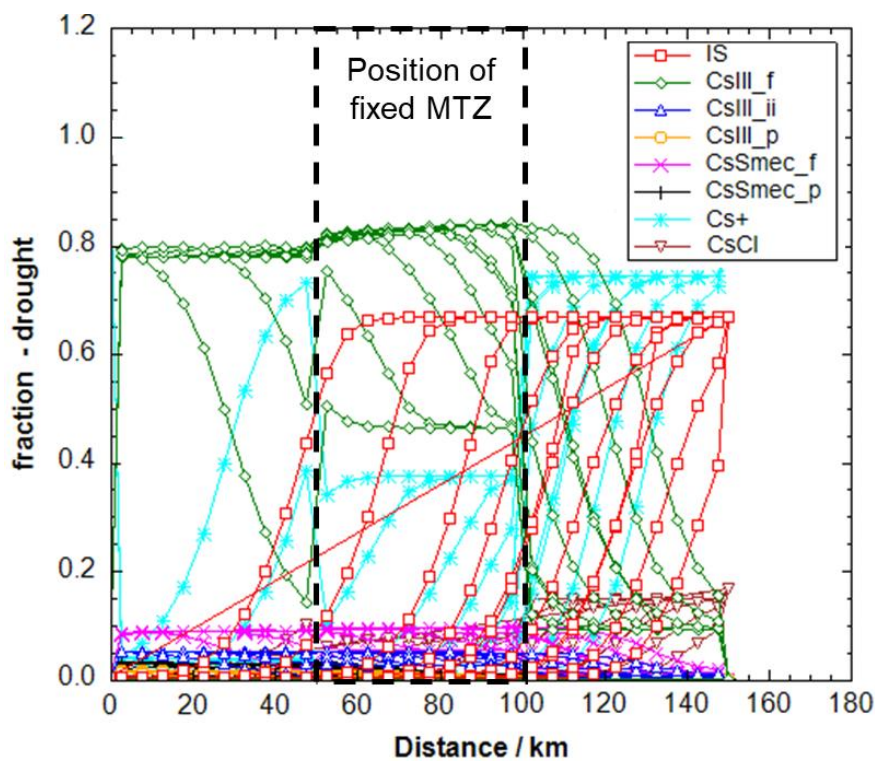


**Figure S4:** Example of one of the outcomes from Model 3 during simulated drought conditions. The column is originally full of freshwater and the seawater endmember starts from the right-hand side to flow inside the column. Different steps of this inflow are plotted simultaneously, each of them indicated by the gradient of the ionic strength (IS), where seawater is represented via  $IS = 0.7 \text{ M}$ . The graph represents the fraction of occupied sites at the modelled clay minerals (Illite:  $Cs_{III\_f}$ ,  $Cs_{III\_ii}$ ,  $Cs_{III\_p}$ ; Smectite:  $Cs_{Smec\_f}$  and  $Cs_{Smec\_p}$ ) and dissolved species ( $Cs^+$ ,  $CsCl$ ) compared to total Cs in the system (i.e.,  $Cs_d + C_{sp}$ , which changes every time new equilibriums are reached within the column, with every fresh-/seawater inflow).

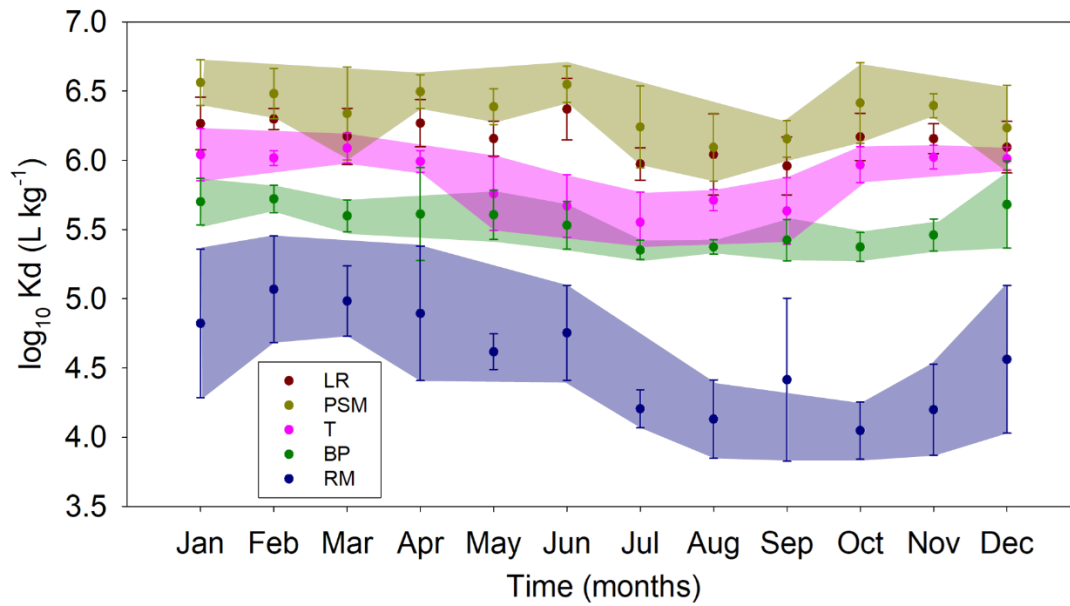


**Figure S5:** Average  $\pm$  SD  $\log_{10}$  Kd values per month during 4-years monitoring at five fluvial sites in the Lot-Garonne watershed. Shaded areas are to guide the eye. Fluvial sites correspond to: La Réole (LR\_Gar-70km), Port-Sainte-Marie (PSM\_Gar-135km), Temple (T\_Lot-135km), Boisse-Penchot (BP\_Lot-235km) and Riou Mort (RM\_Rio-250km).

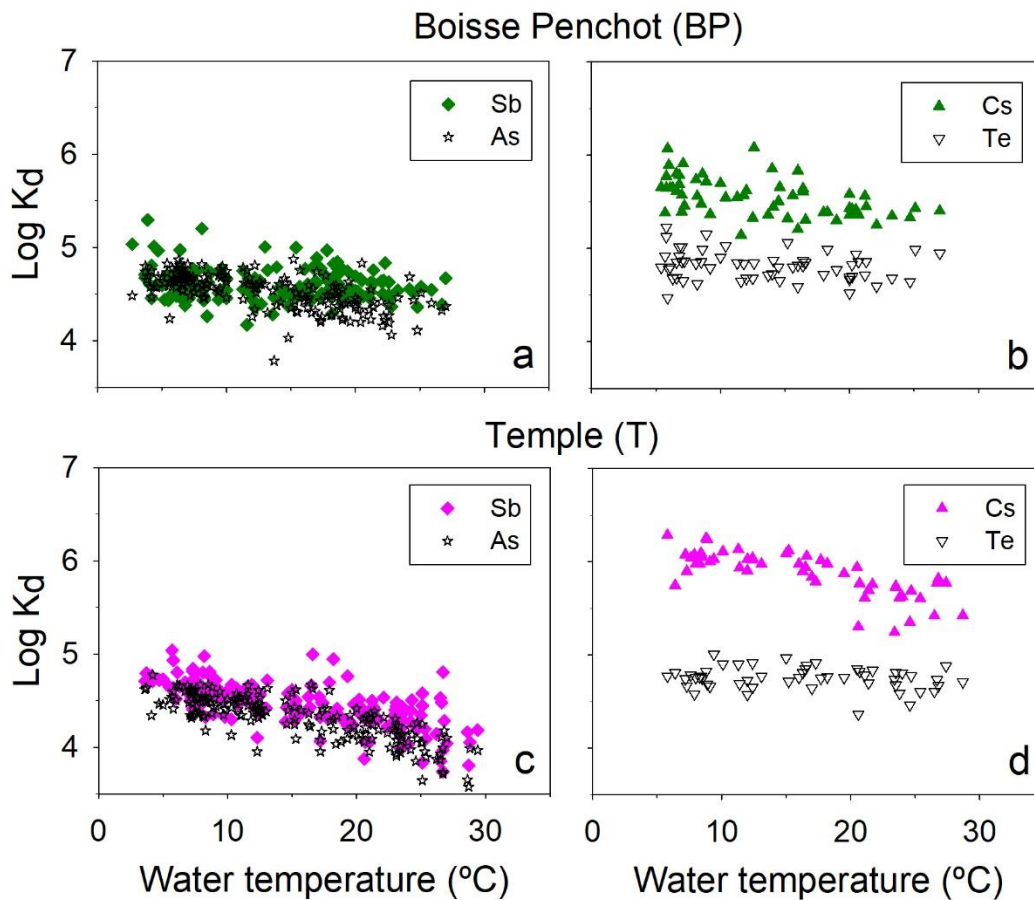


**Figure S6:** Dependency of  $\log_{10}$  Kd values and water temperature at Boisse Penchot (a,b; BP\_Lot-235km) and Temple (c,d; T\_Lot-135km). Data for Sb and As (a,c) from a 14-year time series (2003 – 2016; Gil-Díaz et al. 2018) as well as for Cs and Te (b,d) from a 4-year time series (2014-2017; this work and Gil-Díaz et al. 2019) are shown.

**Table S1:** Composition of the simulated solutions used during the modelling approach. Freshwater and seawater solutions are simplified via the following elemental composition, including pH and salinity.

Elemental composition (mg/l)	Simulated freshwater (pH: 7.27, S: 0.008)	Simulated seawater (pH: 8.2, S: 34.1)
Ca	15	409
Cl*	7	19162
Cs	0.00001	0.0003
K	3	395
Mg	4	1278
Na	6	10679
Rb	0.0001	0.0001
S(+6)	11	2680
Si	7	0.001
Sr	15	7.5

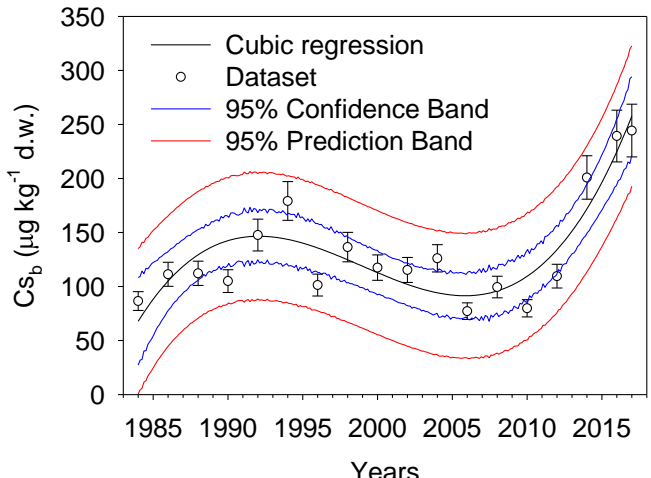
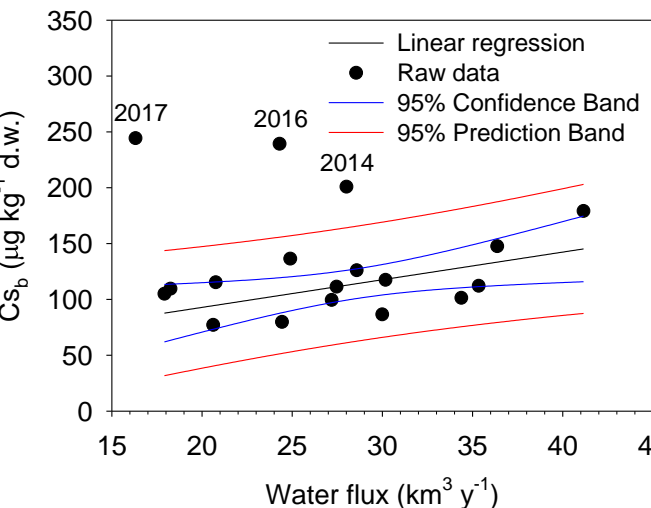
\*Cl is used as the charge balance anion during the calculations

**Table S2:** Summary of the cation-exchange parameters used during model simulations.

Parameters	Illite (Bradbury and Baeyens 2000)	Smectite (Missana et al. 2014)
<b>Type I sites (FES – T1)</b>	$\text{Log}_{\text{Cs}/\text{NaK}} = 7.0$ $\text{Log}_{\text{Cs}/\text{KK}} = 4.6$ $\text{Log}_{\text{Cs}/\text{NH}_4^+\text{K}} = 3.5$	$\text{Log}_{\text{Cs}/\text{NaK}} = 7.59 \pm 0.15$ $\text{Log}_{\text{Cs}/\text{KK}} = 5.15 \pm 0.15$ $\text{Log}_{\text{Cs}/\text{CaK}} = 14.41 \pm 0.17$
<b>Type – II sites (T2)</b>	$\text{Log}_{\text{Cs}/\text{NaK}} = 3.6$ $\text{Log}_{\text{Cs}/\text{KK}} = 1.5$	-
<b>Planar sites (T3)</b>	$\text{Log}_{\text{Cs}/\text{NaK}} = 1.6$ $\text{Log}_{\text{Cs}/\text{KK}} = 0.5$	$\text{Log}_{\text{Cs}/\text{NaK}} = 1.68 \pm 0.15$ $\text{Log}_{\text{Cs}/\text{KK}} = 1.16 \pm 0.15$ $\text{Log}_{\text{Cs}/\text{CaK}} = 3.02 \pm 0.15$
<b>Solid characteristics</b>	CEC = 0.20 eq/kg  <i>Site densities :</i> Illite (T1) = $5.10^{-4}$ eq/kg Illite (T2) = $4.10^{-2}$ eq/kg Illite (T3) = $1.6.10^{-1}$ eq/kg	CEC = 30.91 $\mu\text{eq}/\text{m}^2$ (1.02 eq/kg) BET = 33 $\text{m}^2/\text{g}$ <i>Site densities :</i> Ca-smectite (T1) = $3.5.10^{-3}$ $\mu\text{eq}/\text{m}^2$ Ca-smectite (T3) = 30.91 $\mu\text{eq}/\text{m}^2$ K-smectite (T1) = $1.3.10^{-2}$ $\mu\text{eq}/\text{m}^2$ K-smectite (T3) = 30.91 $\mu\text{eq}/\text{m}^2$

**Table S3:** Statistical approaches to identify  $Cs_b$  bioaccumulation trends in the historical dataset of 34 years (LF\_85km), and its correlation with the water basin discharge. Visual representations (graphs) are included, together with the obtained regression equations (with standard error of the prediction band in brackets), significance of the equation parameters, significance of the correlation ( $R$  value), and normality tests for the datasets used.

	<b>Graphical representation</b>	<b>Statistical information</b>
<b>Linear regression on dataset &lt; 2010 (short dataset)</b>		<p><b>Regression equation and determination coefficient:</b></p> $y = y_0 + ax$ $y = 1640 (\pm 1840) - 0.76 (\pm 0.92) x \quad (R = 0.233)$ <p><b>Significance of parameters:</b>  <math>p\_value(y_0)</math>: 0.39 (not passed)  <math>p\_value(a)</math>: 0.42 (not passed)</p> <p><b>Normality test:</b>            Shapiro-Wilk test: <math>p\_value</math> of 0.49 (passed)</p>
<b>Linear regression on full dataset (1984 – 2017)</b>		<p><b>Regression equation and determination coefficient:</b></p> $y = y_0 + ax$ $y = - 4460 (\pm 2100) + 2.29 (\pm 1.05) x \quad (R = 0.479)$ <p><b>Significance of parameters:</b>  <math>p\_value(y_0)</math>: 0.05 (passed)  <math>p\_value(a)</math>: 0.04 (passed)</p> <p><b>Normality test:</b>            Shapiro-Wilk test: <math>p\_value</math> of 0.60 (passed)</p>

<p><b>Cubic regression on full dataset (1984 – 2017)</b></p>	 <p>A line graph showing the concentration of <math>Cs_b</math> (in <math>\mu\text{g kg}^{-1}</math> d.w.) on the y-axis (ranging from 0 to 350) against years on the x-axis (ranging from 1985 to 2015). The plot includes a black line for cubic regression, open circles for the dataset, a blue shaded area for the 95% confidence band, and a red shaded area for the 95% prediction band. The data shows a fluctuating trend with a general upward trend towards the end of the period.</p>	<p><b>Regression equation and determination coefficient:</b></p> $y = y_0 + ax + bx^2 + cx^3$ $y = -3.36 \cdot 10^8 (\pm 5.75 \cdot 10^7) + 5.04 \cdot 10^5 (\pm 8.62 \cdot 10^4) x - 252 (\pm 43) x^2 + 0.04 (\pm 0.01) x^3 \quad (R = 0.894)$ <p><b>Significance of parameters:</b>  <math>p\_value(y_0)</math>: &lt;0.0001 (passed), <math>p\_value(a)</math>: &lt;0.0001 (passed),  <math>p\_value(b)</math>: &lt;0.0001 (passed), <math>p\_value(c)</math>: &lt;0.0001 (passed)</p> <p><b>Normality test:</b>  Shapiro-Wilk test: <math>p\_value</math> of 0.48 (passed)</p>
<p><b>Linear regression between <math>Cs_b</math> and the watershed discharge (1984 – 2017)</b></p>	 <p>A scatter plot showing the concentration of <math>Cs_b</math> (in <math>\mu\text{g kg}^{-1}</math> d.w.) on the y-axis (ranging from 0 to 350) against water flux (in <math>\text{km}^3 \text{y}^{-1}</math>) on the x-axis (ranging from 15 to 45). The plot includes a black line for linear regression, solid black circles for raw data, a blue shaded area for the 95% confidence band, and a red shaded area for the 95% prediction band. Three data points are specifically labeled with their years: 2017, 2016, and 2014.</p>	<p><b>Regression equation and determination coefficient:</b></p> $y = y_0 + ax$ $y = 43.3 (\pm 27.8) + 2.47 (\pm 0.95) x \quad (R = 0.600)$ <p><b>Significance of parameters:</b>  <math>p\_value(y_0)</math>: 0.15 (not passed)  <math>p\_value(a)</math>: 0.02 (passed)</p> <p><b>Normality test:</b>  Shapiro-Wilk test: <math>p\_value</math> of 0.39 (passed)</p>

**Table S4:** Spearman correlations ( $r$ ) for water discharge ( $Q$ ), suspended particulate matter (SPM), water temperature (Temp), dissolved Cs ( $C_{sd}$ ), particulate Cs ( $C_{sp}$ ) and Th-normalized Cs ( $C_{sp}/Th_p$ ) at the five sampled sites: in table A (LR\_Gar-70km and PSM\_Gar-135km), in table B (T\_Lot-135km and BP\_Lot-235km) and in table C (RM\_Rio-250km). The first number corresponds to the correlation coefficient, the second number (in italics) is the  $p$ -value. Significant correlations ( $p$ -value  $\leq 0.05$ ) are highlighted in black and bold format.

A	SPM (mg/l)	Q (m <sup>3</sup> /s)	Temp (°C)	C <sub>sp</sub> (mg/kg)	Cs/Th	C <sub>sd</sub> (ng/L)	
SPM (mg/l)	-	<b>0.63</b> <i>2.0e-7</i>	-0.22 <i>0.09</i>	0.22 <i>0.10</i>	-0.03 <i>0.85</i>	<b>-0.48</b> <i>1.6e-4</i>	La Réole (LR)
Q (m <sup>3</sup> /s)	<b>0.64</b> <i>2.0e-7</i>	-	<b>-0.68</b> <i>2.0e-7</i>	<b>0.36</b> <i>5.8e-3</i>	0.19 <i>0.17</i>	<b>-0.33</b> <i>0.01</i>	
Temp (°C)	-0.18 <i>0.18</i>	<b>-0.61</b> <i>2.3e-7</i>	-	<b>-0.46</b> <i>2.6e-4</i>	-0.24 <i>0.08</i>	0.06 <i>0.65</i>	
C <sub>sp</sub> (mg/kg)	0.22 <i>0.09</i>	<b>0.37</b> <i>4.0e-3</i>	-0.24 <i>0.06</i>	-	<b>0.78</b> <i>2.0e-7</i>	0.03 <i>0.82</i>	
Cs/Th	0.24 <i>0.08</i>	<b>0.43</b> <i>1.2e-3</i>	<b>-0.28</b> <i>0.04</i>	<b>0.71</b> <i>2.0e-7</i>	-	<b>0.28</b> <i>0.03</i>	
C <sub>sd</sub> (ng/L)	<b>-0.36</b> <i>6.6e-3</i>	<b>-0.44</b> <i>7.6e-4</i>	<b>0.29</b> <i>0.03</i>	-0.19 <i>0.16</i>	-0.05 <i>0.75</i>	-	
<b>Port Sainte Marie (PSM)</b>							

B	SPM (mg/l)	Q (m <sup>3</sup> /s)	Temp (°C)	C <sub>sp</sub> (mg/kg)	Cs/Th	C <sub>sd</sub> (ng/L)	
SPM (mg/l)	-	<b>0.33</b> <i>2.0e-7</i>	-0.23 <i>0.10</i>	0.16 <i>0.21</i>	0.19 <i>0.16</i>	<b>-0.28</b> <i>0.03</i>	Temple (T)
Q (m <sup>3</sup> /s)	<b>0.44</b> <i>3.2e-69</i>	-	<b>-0.63</b> <i>1.7e-7</i>	<b>0.52</b> <i>1.9e-5</i>	0.12 <i>0.36</i>	<b>-0.35</b> <i>6.6e-3</i>	
Temp (°C)	-0.19 <i>0.15</i>	<b>-0.74</b> <i>2.0e-7</i>	-	<b>-0.77</b> <i>2.0e-7</i>	-0.21 <i>0.15</i>	<b>0.57</b> <i>1.1e-5</i>	
C <sub>sp</sub> (mg/kg)	0.21 <i>0.11</i>	<b>0.50</b> <i>5.1e-5</i>	<b>-0.40</b> <i>1.7e-3</i>	-	<b>0.55</b> <i>1.4e-5</i>	<b>-0.27</b> <i>0.04</i>	
Cs/Th	0.24 <i>0.08</i>	<b>0.45</b> <i>4.7e-4</i>	<b>-0.29</b> <i>0.04</i>	<b>0.80</b> <i>2.0e-7</i>	-	<b>0.27</b> <i>0.05</i>	
C <sub>sd</sub> (ng/L)	<b>-0.45</b> <i>2.2e-4</i>	<b>-0.63</b> <i>5.8e-9</i>	<b>0.56</b> <i>3.9e-6</i>	<b>-0.53</b> <i>1.2e-5</i>	<b>-0.36</b> <i>5.3e-3</i>	-	
<b>Boisse Penchot (BP)</b>							

C	SPM (mg/l)	Q (m <sup>3</sup> /s)	Temp (°C)	C <sub>sp</sub> (mg/kg)	Cs/Th	C <sub>sd</sub> (ng/L)	
SPM (mg/l)	-	<b>0.62</b> <i>2.0e-7</i>	-0.14 <i>0.30</i>	<b>0.62</b> <i>1.4e-7</i>	<b>0.32</b> <i>0.02</i>	<b>-0.42</b> <i>9.4e-4</i>	Riou Mort (RM)
Q (m <sup>3</sup> /s)	-	-	<b>-0.58</b> <i>2.2e-6</i>	<b>0.67</b> <i>2.0e-7</i>	0.25 <i>0.07</i>	<b>-0.80</b> <i>2.0e-7</i>	
Temp (°C)	-	-	-	-0.22 <i>0.10</i>	-0.06 <i>0.69</i>	<b>0.54</b> <i>2.1e-5</i>	
C <sub>sp</sub> (mg/kg)	-	-	-	-	<b>0.60</b> <i>2.0e-6</i>	<b>-0.66</b> <i>2.0e-7</i>	
Cs/Th	-	-	-	-	-	-0.24 <i>0.08</i>	
C <sub>sd</sub> (ng/L)	-	-	-	-	-	-	

**Table S5:** Non exhaustive summary of experimental studies reporting  $K_d$  values for Cs sorption onto single-mineral surfaces.

Experimental conditions	$K_d$ values	Reference
Clay minerals		
Three homo-ionic smectites (Na-, K-, Ca-smectite), in a wide pH range (2 – 11), at varying ionic strength (0.001 M to 1 M) and Cs concentrations ( $10^{-10}$ – $10^{-3}$ M).	Case of Na-smectite for pH > 5 at: 0.1 M NaClO <sub>4</sub> : 501 L/kg (log $K_d$ ~ 2.7 L/kg) 0.01 M NaClO <sub>4</sub> : 5011 L/kg (log $K_d$ ~ 3.7 L/kg)	Missana et al. 2014
Basic pH (8 and 10), sorption of Cs ( $10^{-11}$ – $10^{-5}$ M) onto montmorillonite nanoparticles	Colloidal: ~10 000 L/kg Sedimented: ~ 1 000 L/kg	Iijima et al. 2010
Cs sorption (0.94 and 4.29 mM) onto Ca-montmorillonite, in the presence of Sr <sup>2+</sup> competition. 20 g/L of solid/liquid ratio, in 0.001 M NaCl, at adjusted pH between 4 – 9.	~140 - 300 L/kg *	Gutierrez and Fuentes 1996
10 g/L solid to liquid ratio, non-specified ionic strength but Cs concentrations of $10^{-2}$ M and regulated pH between 3 and 8	Kaolinite < 10 L/kg Sepiolite ~ 25 L/kg Zeolite (fine) ~ 150 L/kg Bentonite ~ 225 L/kg Zeolite (coarse) ~ 250 L/kg at pH ~7	Bayülken et al. 2011
Other surfaces		
Unspecified solid/liquid ratio (“0.1 g of magnetite in a certain volume”), and unspecified ionic strength (assumed freshwater = 0.05 M) at pH ~8.	Ferrite ~300 L/kg Natural magnetite ~120 L/kg	Sheha and Metwally 2007
> 20 g/L of humic dosage, at pH between 7 and 9, for an initial dose of ~ 6.7 mg/L of Cs.	~200 kg/L*	Khan and Bagla, 2022
0.25 g/L of nanoparticles, 25°C and $10^{-2}$ M CsCl, probably at pH 6	TiO <sub>2</sub> : 124.59 L/kg	Metwally et al. (2007)
Parameters for a reactive transport study.	Quartz: 0 L/kg Feldspars: 106 L/kg in feldspars Biotite: 317 L/kg	Voutilainen et al. 2017

\*Calculated values from presented data